

# Transverse dynamical magnetic susceptibilities from regular static density functional theory: Evaluation of damping and $g$ -shifts of spin-excitations

Samir Lounis<sup>†,\*</sup>, Manuel dos Santos Dias, and Benedikt Schwefflinghaus  
*Peter Grünberg Institut and Institute for Advanced Simulation,  
 Forschungszentrum Jülich, 52425 Jülich & JARA, Germany*

The dynamical transverse magnetic Kohn-Sham susceptibility calculated within time-dependent density functional theory shows a fairly linear behavior for a finite energy window. This observation is used to propose a scheme where the computation of this quantity is greatly simplified. Regular simulations based on *static* density functional theory can be used to extract the dynamical behavior of the magnetic response function. Besides the ability to calculate elegantly damping of magnetic excitations, we derive along the way useful equations giving the main characteristics of these excitations: effective  $g$ -factors and the resonance frequencies that can be accessed experimentally using inelastic scanning tunneling spectroscopy or spin-polarized electron energy loss spectroscopy.

## I. INTRODUCTION

Probing spin excitations on surfaces is a major focus of recently developed state of the art experimental techniques: spin polarized electron energy loss spectroscopy (SPEELS) [1, 2] or inelastic scanning tunneling spectroscopy (ISTS) [3–10] allow, for example, to map partly the excited spectra of thin films and even nano-structures down to single adatoms on surfaces. All information on spin-excitations is encoded in the magnetic response of a material, but once probed experimentally it is dressed up differently depending on the measurement technique. This explains the theoretical efforts, thriven by these experimental achievements, in developing methods that permit to simulate the dynamical transverse magnetic susceptibility,  $\chi$ , that, in linear response, describes the amplitude of the transverse spin motion produced by an external magnetic field of frequency  $\omega$  [11–19]. The excitations spectrum hinges on the details of the electronic structure of the probed material, hybridization of electronic states and magnetization.

Within SPEELS or ISTS, surface spin waves or localized spin excitations are excited via an exchange scattering process involving either a spin-polarized monochromatic electron beam or a tunneling current that interact with the sample. A gap in the dispersion curve of the spin waves (difficult to observe with actual SPEELS) or in the ISTS signal is the signature of symmetry breaking induced by spin-orbit coupling (SOC) or by an external magnetic field  $B$ . For single adatoms on non-magnetic substrates, the observed resonances, experimentally and theoretically, are located at the Larmor energy given by  $g_{\text{eff}}\mu_B B$  with an effective spectroscopic splitting factor surprisingly different from 2 [3–5, 7, 8, 16, 19, 20]. The lifetime (damping)

of the spin-excitations and  $g$ -shifts are the results of the coupling to Stoner (electron-hole pairs) excitations that change depending on the magnitude of the applied magnetic field [5, 16, 20, 21]. In fact,  $g$ -shifts were recognized since the early days of ferromagnetic resonance spectroscopy (FMR) [22] and were related to the presence of SOC [23–25]. Contrary to FMR, ISTS probes the magnetic response locally instead of the full system. In this particular case, Mills and Lederer [26] predicted that  $g$  can be different from 2 even without SOC. Indeed, during spin-precession, the surrounding bath of electrons are perturbed and spin-currents are emitted. The local response naturally differs from the global response as expected in the spin-pumping context.

To calculate dynamical magnetic quantities from ab initio, one uses either time-dependent density functional theory (TD DFT) [27] or many-body perturbation theory (MBPT) coupled to DFT [28]. Since the calculation of such quantities is a computational burden, their accessibility is limited [29]. The goal of our manuscript is to present an attractive scheme wherein simple equations derived within TD DFT allow to calculate dynamic properties just by computing *static* quantities defined at the Fermi energy; this is reasonable within linear response theory. Thus, our formulation can be implemented without tremendous efforts.

A byproduct of our analysis is a simple formulation of the damping, local or non-local in space, of the spin-excitations. We note that the relation between the damping and the electronic structure has been predicted earlier [20, 26]. Moreover, several proposals (see e.g. Refs. [30–32]) have been made to calculate the phenomenological damping parameter,  $\lambda$ , used to couple the precession of the moment to a reservoir when solving Landau-Lifshitz-Gilbert (LLG) equations [33]. Calculations based on first-principles were also performed in Refs. [34–38], with a focus on  $\lambda$  but not on the full magnetic response function.

<sup>†</sup>Electronic address: s.lounis@fz-juelich.de

In our work, we derive furthermore a physically transparent form of the effective  $g$ -factor defining the response of the system to an external magnetic field. We relate its shift to the electronic structure and more precisely to the local density of states at the Fermi energy. It is interesting to note that Qian and Vignale [39] recognized in their derivation of the spin-wave dynamics from TD DFT a dynamic term and a ‘‘Berry curvature’’ correction, which we believe can be connected to the  $g$ -shift mentioned earlier [51].

We note that in the context of Kondo impurities  $g$ -shifts were also predicted many years ago [40], which was recently used to interpret experimental data extracted with ISTS [10, 41, 42]. Using first-order perturbation theory in the weak coupling regime of a spin to the surrounding electronic bath, the shift in  $g$  was shown to be proportional to  $Jn(E_F)$ , where  $J$  describes an  $s$ - $d$  type of interaction between a localized moment with the conduction electron and  $n(E_F)$  is the density of states of conduction electrons at the Fermi energy. We stress that the latter is rather similar to our concept of renormalization of  $g$  due to the electronic structure derived within TD DFT.

## II. METHOD AND FRAMEWORK

The transverse dynamical magnetic susceptibility connecting the transverse magnetization to an infinitesimal transverse dynamical magnetic field is evaluated within TD DFT by solving the Dyson-like equation:

$$\chi = \frac{\chi_0}{1 - U\chi_0} \quad (1)$$

in a matrix notation.  $U$  is the exchange and correlation kernel, which is assumed to be local in space and adiabatic.  $\chi_0$  is the Kohn-Sham susceptibility whose imaginary part describes the density of Stoner excitations and can be written as a convolution of Green functions connecting the radial points  $\vec{r}$  and  $\vec{r}'$  centered respectively around sites  $i$  and  $j$ :

$$\chi_0^{ij}(\vec{r}, \vec{r}'; \omega) = -\frac{1}{\pi} \int dz f(z) [G_{ij}^\downarrow(\vec{r}, \vec{r}'; z + \omega) \text{Im} G_{ji}^\uparrow(\vec{r}', \vec{r}; z) + \text{Im} G_{ij}^\downarrow(\vec{r}, \vec{r}'; z) G_{ji}^\uparrow(\vec{r}', \vec{r}; z - \omega)],$$

where  $f(z)$  is the Fermi distribution function,  $G$  and  $G^-$  represent the retarded and advanced one-particle Green functions connecting atomic sites  $i$  and  $j$  and  $\text{Im} G = \frac{1}{2i}(G - G^-)$ . The assessment of  $\chi_0$  requires to compute Green functions at energies  $z$ ,  $z + \omega$  and  $z - \omega$ . Also usual contour deformations when calculating the integral are not possible since there is a convolution of Green functions that are not analytical in the same complex half plane.

We evaluated the Kohn-Sham susceptibility for several systems utilizing our recently developed method [16, 19,

21] based on the Korringa-Kohn-Rostoker Green function method [43]. In this scheme, the Green functions are projected on a chosen basis and the magnetic response to a spherically symmetric or site-dependent magnetic field is assumed. Within this approach  $U$  simplifies to a single number per magnetic atom. In this case, the quantity of interest is the spherical part of the magnetic susceptibility  $\bar{\chi}^{ij}(r, r'; \omega) = \sum_{LL_1} \chi^{iLL_1jL_1L}(r, r'; \omega)$ .

In Figs. 1(a), 1(b) and 1(c), we plot the imaginary and real parts of  $\chi_0$  for Cr, Mn, Fe and Co single adatoms on Cu(111) and the imaginary part of  $\chi_0$  for 8 Co monolayers on Cu(001). In the latter case, the layer-resolved quantity is shown for the four last Co surface layers. Obviously, the imaginary and real parts of  $\chi_0$  are rather linear with frequency. This linear regime defines the domain of applicability of the scheme proposed in this contribution, i.e., it is limited to few tens of meV up to a couple of hundred meV depending on the investigated material.

In this linear regime, the transverse Kohn-Sham susceptibility can thus be written in a Taylor expansion,

$$\chi_0(\omega) = \text{Re} \chi_0(0) + (\text{Re} S + i \text{Im} S) \omega + O(\omega^2), \quad (3)$$

where the slope  $S$  is given by  $\frac{\partial \chi_0}{\partial \omega}$  and  $\text{Re} \chi_0(0)$  is a Fermi-sea like term since it involves an energy integration up to the Fermi energy of a convolution of Green functions (see Eq. 2). We demonstrate that the slopes defining the linearity of  $\chi_0$  can be determined from one single DFT-based calculation. Once  $\chi_0$  is known, the full-susceptibility  $\chi$  can be evaluated after solving a Dyson-like equation (Eq. 1).

For simplification, we assume that the systems of interest are magnetically collinear. Also, SOC is set aside allowing to decouple the longitudinal excitations from the transverse ones. However, one can use an external magnetic field to mimic the energy gap induced by SOC, which is of the order of the magnetic anisotropy energy. In other words, the magnetic field shifts the position of the resonances, thereby picking up electron-hole excitations that affect the corresponding lifetimes. In that case the gap is given by  $g\mu_B B$ . Both procedures lead to about the same lifetimes [5] within a tight-binding scheme [17] or using TD DFT including SOC [44].

## III. DERIVATION AND RESULTS

Since  $G(z \pm \omega) = G(z) \mp G(z)\omega G(z \pm \omega)$  and taking the limit of  $\omega \rightarrow 0$  we find that  $G(z \pm \omega) \simeq G(z) \mp \omega G(z)G(z)$  in matrix notation. We know that  $\frac{\partial G(z \pm \omega)}{\partial \omega} \simeq \mp G(z)G(z) \simeq \pm \frac{dG(z)}{dz}$ . Therefore for small  $\omega$ ,

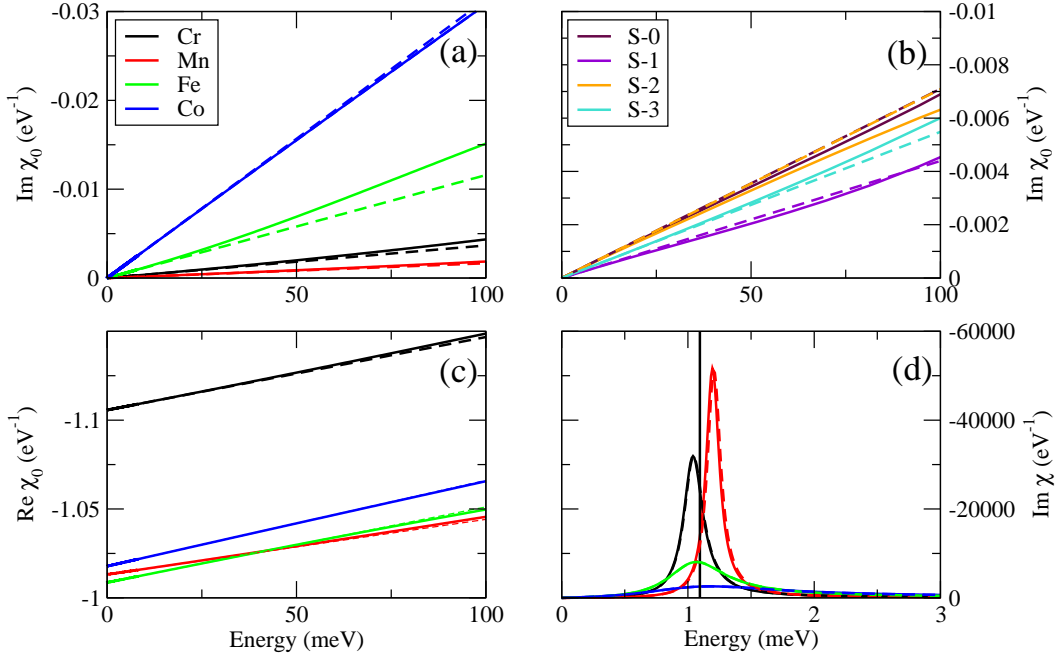


FIG. 1: The spherical component of the imaginary part of the transverse dynamic Kohn-Sham susceptibility,  $\text{Im } \chi_0$ , shown for two systems: 4 different transition-metal adatoms on a Cu(111) surface (a), and 8 monolayers of Co on a Cu(001) surface, S- $n$  denoting the  $n$ -th layer with respect to the surface (b). The results show a fair linear behavior up to large energies, which is well described by the dashed lines obtained with Eq. 4. As discussed in the text, a linear behavior is also expected for the real part of the Kohn-Sham susceptibility, which is indeed found as depicted in (c) for the case of transition-metal adatoms on a Cu(111) surface. After application of Eq. 4 for the adatoms, the full transverse dynamic susceptibility is recovered (full lines versus dashed lines) in (d).

$$S^{ij}(\vec{r}, \vec{r}') = \frac{i}{2\pi} \left[ \int^{E_F} dz \left( \frac{dG_{ij}^\downarrow(\vec{r}, \vec{r}'; z)}{dz} G_{ji}^\uparrow(\vec{r}', \vec{r}; z) + G_{ji}^{*\downarrow}(\vec{r}', \vec{r}; z) \frac{dG_{ij}^{*\uparrow}(\vec{r}, \vec{r}'; z)}{dz} \right) + G_{ij}^\downarrow(\vec{r}, \vec{r}'; E_F) G_{ij}^{*\uparrow}(\vec{r}, \vec{r}'; E_F) \right] \quad (4)$$

Eq. 4 is among the important results reported in this paper. It shows that extracting the linear behavior of the susceptibility requires an integral along a complex energy contour of a convolution of Green functions that are analytical on the same complex half plane. Therefore usual techniques used in regular methods based on Green functions can be applied (see e.g. Ref. [43]). Also the evaluation of  $dG/dz$  is numerically straightforward and the integral over the energy is evaluated only once, thus the computational costs are dramatically reduced compared to those needed for the evaluation of Eq. 2.

We utilized Eq. 4 to evaluate the Kohn-Sham susceptibilities for the cases mentioned earlier, for instance Cr, Mn, Fe and Co adatoms on Cu(111) surface and Co thin film on Cu(001) surface. The results are shown in Fig. 1 as dashed lines, which fit rather well the overall behavior of  $\chi_0$ . For indication, the slopes obtained for the adatoms are listed in Table I. In Fig. 1(d), we plot the imaginary part of the full transverse dynamical susceptibility using  $\chi_0$  obtained with the regular scheme, i.e. integral given by Eq. 2 (full lines) and with Eqs. 3 and 4 (dashed lines). Also values of  $g_{\text{eff}}$  obtained with both type of calculations are presented in Table I. The agreement is extremely good

	Cr	Mn	Fe	Co
Re $S$ (eV <sup>-2</sup> )	-0.411	-0.310	-0.425	-0.483
Im $S$ (eV <sup>-2</sup> )	-0.037	-0.017	-0.116	-0.313
$\beta$ (eV <sup>-2</sup> )	0.784	0.681	0.858	1.237
$g_{\text{eff}}$	1.89	2.17	1.95	2.14
$g_{\text{eff}}$ (after using Eq. 4)	1.90	2.19	1.95	2.15

TABLE I: Values of the slope of the Kohn-Sham susceptibility, Re  $S$  and Im  $S$ , at small frequencies calculated with Eq. 4 for different adatoms on Cu(111) surface. Those values lead to a good description of the low-energy regime of the Kohn-Sham susceptibility and of the full transverse susceptibility as can be observed in Fig. 1. For instance, values of  $g_{\text{eff}}$  obtained from both schemes are about the same.

which validates our proposal.

For the adatom case and in the linear regime, the imaginary part of  $\chi$  given by

$$\text{Im } \chi = \frac{\text{Im } \chi_0}{[1 - U \text{Re } \chi_0]^2 + [U \text{Im } \chi_0]^2} \quad (5)$$

can be rewritten as

$$\text{Im } \chi = \frac{\omega \text{Im } S}{[1 - U(\omega \text{Re } S + \text{Re } \chi_0(0))]^2 + (U\omega \text{Im } S)^2}, \quad (6)$$

which defines the density of magnetic excitations, i.e. it gives the theoretical spectrum corresponding to the experimental measurements.

In Eq. 6 one recognizes similarities with the regular Dyson equations allowing to compute Green functions. For example, an orbital originally located at  $E_0$ , broadens and experiences a shift after hybridization with the electronic background. The latter can be described via the self-energy  $\Sigma$  and the corresponding imaginary part of the Green function reads

$$\text{Im } G = \frac{\text{Im } \Sigma}{([E - E_0 - \text{Re } \Sigma]^2 + [\text{Im } \Sigma]^2)}. \quad (7)$$

One deduces that  $\chi_0$  acts as a self-energy with an imaginary part defining the lifetime of the excitations described by  $\chi$  while the real part of  $\chi_0$  defines its energy-shift.

### A. Imaginary part of the slope of $\chi_0$

It is interesting to note that the imaginary part of the slope  $S$  can be deduced in a transparent form that reads

$$\text{Im } S^{ij}(\vec{r}, \vec{r}') = -\pi n_{ij}^\downarrow(\vec{r}, \vec{r}'; E_F) n_{ji}^\uparrow(\vec{r}', \vec{r}, E_F), \quad (8)$$

where  $n_{ij}^\sigma(\vec{r}, \vec{r}'; E) = -\frac{1}{2\pi i} (G_{ij}^\sigma(\vec{r}, \vec{r}'; E) - G_{ij}^{*\sigma}(\vec{r}, \vec{r}'; E))$  and  $\sigma \in \{\uparrow, \downarrow\}$ . Eq. 8 is compelling and useful: the imaginary part of the change of  $\chi_0$  at small frequencies is related to the density matrix for each spin channel at the Fermi

energy. Im  $S$  can thus be considered as a Fermi-surface-like term. If  $\vec{r} = \vec{r}'$ , i.e., the susceptibility is local in space and depends on the product of energy-dependent charge density of opposite spin-character. This is the second important result of this work. The lifetime of the excitation and, thus, the damping can be calculated exactly after a one-shot calculation from a regular static DFT run without even having to perform an energy integration. We propose to use this damping directly on top of the adiabatic approach usually utilized to extract the magnetic exchange interactions (see e.g. Refs. [45–47]) and the related dispersion of spin-waves or the localized spin-excitations spectra (e.g. Refs. [48–50]). However, one has to keep in mind that Stoner excitation will impact on the position of spin waves resonances via the real part of the Kohn-Sham susceptibility, which will be the topic of the next paragraph.

We note that Eq. 8 reduces to

$$\text{Im } \bar{S}^{ij} = -\pi \sum_{LL_1} n_{LL_1}^{ij\downarrow}(E_F) n_{L_1L}^{ij\uparrow}(E_F) \quad (9)$$

if we use the framework presented in Ref. [16], where a projection of the Green functions on the  $d$  states is made and the response to a spherically symmetric or site-dependent magnetic field is assumed.

Eqs. 8 or 9 have paramount physical implications: The way the minority or majority spin-levels intersect the Fermi energy defines the damping of the excitations in terms of the product of density of states of opposite spin character. This explains for example that Fe and Co adatoms on several surfaces (e.g. Cu(001), Cu(111) and Ag(111) surfaces) have broad resonances in their excitation spectra since their minority-spin local density of states experiences a resonance close to the Fermi energy contrary to Mn and Cr adatoms on the same surfaces, which have much sharper resonances because the Fermi level lies between the majority and minority states [5, 16, 21]. Considering that scanning tunneling microscopy can be used to map the spin-polarized local density of states at the Fermi energy, an experimental estimate of the damping can be provided via Eq. 8.

### B. Real part of the slope of $\chi_0$

Compared to the imaginary part, the real part of  $S$  is, however, not easy to simplify. To obtain a simple form of the real part, both sides of Eq. 4 are multiplied by the exchange splitting potential,  $B^i$  from the right and  $B^j$  from the left, integrated over  $d\vec{r}$ ,  $d\vec{r}'$ , and summed up over  $i$  and  $j$ , where  $B^i$  is given by the difference between the potentials of each spin channel ( $V^\uparrow - V^\downarrow$ ) for atom  $i$ . We make use of  $G^\uparrow = G^\downarrow + G^\downarrow B G^\uparrow$  and define the total moment of the system  $M$  in order to reduce

$\sum_{ij} \int d\vec{r} d\vec{r}' B^i(\vec{r}) S^{ij}(\vec{r}, \vec{r}') B^j(\vec{r}')$  (at  $\omega=0$ ) to a sum rule:

$$\sum_{ij} B^i S^{ij} B^j = -M + \sum_j G_{jj}^{*\uparrow}(E_F) B^j - \sum_i B^i G_{ii}^{\downarrow}(E_F) + \frac{1}{2\pi i} B^i (G_{ij}^{\downarrow}(E_F) G_{ij}^{*\uparrow}(E_F)) B^j, \quad (10)$$

in a matrix notation. Interestingly, the calculation of the total magnetic moment involves an energy integration up to the Fermi energy and thus can be identified as a Fermi-sea-like contribution to the sum rule while the remaining terms are Fermi-surface-like contributions.

In the case of a single magnetic adatom deposited on a non-magnetic substrate and within the spherical approximation defined earlier, Eq. 10 becomes

$$\bar{S}^{ii} = -\frac{1}{B_i} M_i \frac{1}{B_i} - \frac{1}{2\pi i} \sum_L \left[ \frac{1}{B_i} G_{ii,LL}^{*\uparrow}(E_F) - G_{ii,LL}^{\downarrow}(E_F) \frac{1}{B_i} \right] + \frac{1}{2\pi i} \sum_{LL_1} (G_{ii,LL_1}^{\downarrow}(E_F) G_{ii,L_1L}^{*\uparrow}(E_F)), \quad (11)$$

and for instance, the real part is given by

$$\text{Re} \bar{S}^{ii} = -\frac{1}{B_i} M_i \frac{1}{B_i} - \frac{n^i(E_F)}{2B_i} + \text{Im} \left[ \frac{1}{2\pi} \sum_{LL_1} (G_{ii,LL_1}^{\downarrow}(E_F) G_{ii,L_1L}^{*\uparrow}(E_F)) \right], \quad (12)$$

where we have replaced  $\text{Im} \frac{1}{\pi} \sum_L [G_{ii,LL}^{*\uparrow}(E_F) - G_{ii,LL}^{\downarrow}(E_F)]$  by the total density of states at the Fermi energy  $n^i(E_F)$ .  $\text{Re} S$  depends on properties defined at the Fermi energy, Fermi-surface-like terms, and on an energy integrated term, the magnetic moment, which defines a Fermi-sea-like contribution. Unlike  $\text{Im} S$ ,  $\text{Re} S$  is in this particular case a complicated combination of parameters. It hinges on the magnetization, the exchange splitting, the density of states at the Fermi energy as well as the real part of a product of Green functions of opposite spin.

### C. Resonance energy, $g$ -values and spin-excitation's lifetime of single adatoms

In this model, the resonance energy for the single adatom case,  $\omega_{\text{res}}$ , in the excitation spectrum is given by the extremum of  $\text{Im} \chi$ , i.e.  $\frac{\partial \text{Im} \chi}{\partial \omega} = 0$ . From Eq. 6 we find

$$\omega_{\text{res}} = \frac{|\frac{1}{U} - \text{Re} \bar{\chi}_0(0)|}{\sqrt{\text{Re} S^2 + \text{Im} S^2}}. \quad (13)$$

Thus, the position of the resonance depends equally on the slope  $S$  as well as on the value of  $\text{Re} \bar{\chi}_0$  at  $\omega = 0$ . Furthermore, the full-width half maximum value, which defines the

spin-excitation's lifetime, turns out to be proportional to  $\omega_{\text{res}}$  and reads

$$\text{FWHM} = 2 \cdot \sqrt{\left( 2 + \frac{\text{Re} S}{\sqrt{(\text{Re} S)^2 + (\text{Im} S)^2}} \right)^2 - 1} \cdot \omega_{\text{res}} \quad (14)$$

If no external magnetic field is applied along the  $z$  direction,  $\text{Re} \bar{\chi}_0(0) = 1/U$  since the Goldstone mode has to be satisfied and consequently  $\omega_{\text{res}} = 0$ . If a magnetic field  $B$  is applied along the  $z$  direction, the effective Larmor energy is given by  $\omega_{\text{res}} = g_{\text{eff}} \mu_B B$  and

$$g_{\text{eff}} = \frac{1}{\mu_B B} \frac{|\frac{1}{U} - \text{Re} \bar{\chi}_0(0)|}{\sqrt{(\text{Re} S)^2 + (\text{Im} S)^2}} \quad (15)$$

describes the response of the system to this field. Results obtained from the previous equation recover naturally the values extracted from Fig. 1(d) and shown in Table I.

Using once more a Taylor expansion of  $\chi_0$  in terms of the applied magnetic field and the sum rule relating  $\chi_0$  to  $U$  at zero-magnetic field we end up with:

$$g_{\text{eff}} \approx g \sqrt{\frac{\beta^2}{(\text{Re} S)^2 + (\text{Im} S)^2}} \quad (16)$$

where  $\beta$  is given by the first two terms of the right-hand side of Eq. 12, i.e., it can be written as

$$\beta = -\frac{1}{B_i} M_i \frac{1}{B_i} - \frac{n^i(E_F)}{2B_i}. \quad (17)$$

This result has important consequences. If the local density of states at the Fermi energy vanishes,  $\text{Im} S$  goes to zero while  $\beta$  converges to  $\text{Re} S$  leading to  $g_{\text{eff}} = 2$ . However, any finite occupation at the Fermi energy, in other words, any metallic behavior will shift  $g$  away from 2. Access to the exchange splitting and the magnetic moment of a material may help to estimate the shift in  $g$  as well as the lifetime of spin-excitations via Eq. 16. Values of  $\beta$  for Cr, Mn, Fe and Co adatoms are presented in Table I.

Besides  $g$ , another quantity describes the spin-dynamics, namely the damping parameter  $\lambda$  encountered in the LLG equations [33]. Several studies were recently devoted to the formulation and computation of the Gilbert damping parameter from realistic electronic structures [31, 34–38]. Here we use Eq. 8 and as an example, we derive the form of  $\lambda$  considering the particular case of a single magnetic impurity. After applying a transverse time-dependent magnetic field  $\vec{B}_t$  on top of the static field  $\vec{B}$  parallel to  $\vec{M}$ , we linearize the LLG equations:

$$\frac{d\vec{M}}{dt} = -\frac{g\mu_B}{\hbar} \vec{M} \times (\vec{B} + \vec{B}_t) - \lambda \frac{g\mu_B}{\hbar |\vec{M}|} \vec{M} \times (\vec{M} \times (\vec{B} + \vec{B}_t)) \quad (18)$$

and relate the induced transverse magnetization to the transverse field via a dynamical transverse susceptibility in

a fashion similar to TD DFT:

$$\chi = -\frac{g\mu_B(1+i\lambda)M}{\omega - g\mu_B B - i\lambda g\mu_B B} \quad (19)$$

whose imaginary part can be compared to Eq. 6 in order to identify  $\lambda$ . We find that

$$\lambda = \text{Im } S, \quad (20)$$

which leads to a formulation of the damping parameter entering the LLG equations. From the previous equation, one deduces once more that a metallic system leads to a finite value of  $\lambda$ .

#### IV. CONCLUSION

In this paper we have derived a simple formula that allows to compute the slope of the dynamical transverse magnetic susceptibility from static DFT calculations. The cost of calculations are then tremendously reduced in comparison with the usual method that permits the calculation of the magnetic response function. We provided a comparison between the two methods and demonstrate their mutual agreement for a reasonable energy window. We applied our formalism to a Co thin film on Cu(111) surface and to 3d adatoms on the same substrate. The Fermi

surface defines the dynamical behavior, which is a reasonable statement within linear response theory. Furthermore, our formulation permits a straightforward interpretation of the origin of damping observed in the measured spin-excitations spectra and the dependence on the electronic structure. Using a simple model, we derived an analytical form for the effective  $g$  value of a single magnetic adatom on a non-magnetic substrate and we explain thereby the origin of its shift by the degree of metallicity or itinerancy. Finally, we suggested a mapping procedure from ab initio to a Heisenberg model used when solving LLG equations. For instance, a form of the Gilbert damping parameter due to Stoner excitations is introduced, which is in agreement with previous proposals.

#### Acknowledgments

We acknowledge discussions with late D. L. Mills, A. T. Costa, P. H. Dederichs and S. Blügel. Research supported by the HGF-YIG Programme VH-NG-717 (Functional nanoscale structure and probe simulation laboratory – Funsilab).

- 
- [1] Kh. Zakeri, Y. Zhang, J. Prokop, T.-H. Chuang, N. Sakr, W. X. Tang, J. Kirschner, *Phys. Rev. Lett.* **104**, 137203 (2010). Kh. Zakeri, T.-H. Chuang, A. Ernst, L. M. Sandratskii, P. Buczek, H. J. Qin, Y. Zhang, J. Kirschner, *Nature Nanotechnology* **8**, 853 (2013).
  - [2] J. Rajeswari, H. Ibach, C. M. Schneider, A. T. Costa, D. L. R. Santos, D. L. Mills, *Phys. Rev. B* **86**, 165436 (2012); J. Rajeswari, H. Ibach, C. M. Schneider, *Phys. Rev. Lett.* **112**, 127202 (2014).
  - [3] A. J. Heinrich, J. A. Gupta, C. P. Lutz, D. M. Eigler, *Science* **306**, 466 (2004); C. F. Hirjibehedin *et al.*, C.-Y. Lin, A. F. Otte, M. Ternes, C. P. Lutz, B. A. Jones, A. J. Heinrich, *Science* **317**, 1199 (2007); C. F. Hirjibehedin, C. P. Lutz, A. J. Heinrich, *Science* **312**, 1021 (2006).
  - [4] T. Balashov, T. Schuh, A. F. Takács, A. Ernst, S. Ostanin, J. Henk, I. Mertig, P. Bruno, T. Miyamachi, S. Suga, and W. Wulfhekel, *Phys. Rev. Lett.* **102**, 257203 (2009).
  - [5] A. A. Khajetoorians, S. Lounis, B. Chilian, A. T. Costa, L. Zhou, D. L. Mills, J. Wiebe, R. Wiesendanger, *Phys. Rev. Lett.* **106**, 037205 (2011); B. Chilian, A. A. Khajetoorians, S. Lounis, A. T. Costa, D. L. Mills, J. Wiebe, R. Wiesendanger, *Phys. Rev. B* **84**, 212401 (2011); A. A. Khajetoorians, T. Schlenk, B. Schweflinghaus, M. dos Santos Dias, M. Steinbrecher, M. Bouhassoune, S. Lounis, J. Wiebe, R. Wiesendanger, *Phys. Rev. Lett.* **111**, 157204 (2013).
  - [6] B. W. Heinrich, L. Braun, J. I. Pascual, K. J. Franke, *Nature Physics* **9**, 765 (2013).
  - [7] B. Bryant, A. Spinelli, J. J. T. Wagenaar, M. Gerrits, A. F. Otte, *Phys. Rev. Lett.* **111**, 127203 (2013); A. Spinelli, B. Bryant, F. Delgado, J. Fernandez-Rossier, A. F. Otte, *Nature Materials* **13**, 782 (2014).
  - [8] F. Donati, Q. Dubout, G. Autès, F. Patthey, F. Calleja, P. Gambardella, O. V. Yazyev, H. Brune, *Phys. Rev. Lett.* **111**, 236801 (2013).
  - [9] I. G. Rau, S. Baumann, S. Rusponi, F. Donati, S. Stepanow, L. Gagnaniello, J. Dreiser, C. Piamonteze, F. Nolting, S. Gangopadhyay, O. R. Albertini, R. M. Macfarlane, C. P. Lutz, B. A. Jones, P. Gambardella, A. J. Heinrich, H. Brune, *Science* **344**, 988 (2014).
  - [10] J. C. Oberg, M. R. Calvo, F. Delgado, M. Moro-Lagares, D. Serrate, D. Jacob, J. Fernandez-Rossier, C. F. Hirjibehedin, *Nature Nanotechnology* **9**, 64 (2014).
  - [11] A. T. Costa, R. B. Muniz, D. L. Mills, *Phys. Rev. B* **70**, 054406 (2004).
  - [12] S. Y. Savrasov, *Phys. Rev. Lett.* **81**, 2570 (1998).
  - [13] M. I. Katsnelson, A. I. Lichtenstein, *J. Phys.: Condens. Matter* **16**, 7439 (2004).
  - [14] P. Buczek, A. Ernst, P. Bruno, L. M. Sandratskii, *Phys. Rev. Lett.* **102**, 247206 (2009); P. Buczek, A. Ernst, L. M. Sandratskii, *Phys. Rev. B* **84**, 174418 (2011).
  - [15] E. Sasioglu, A. Schindlmayr, C. Friedrich, F. Freimuth, S.

- Blügel, Phys. Rev. B **81**, 054434 (2010); E. Sasioglu, C. Friedrich, S. Blügel, Phys. Rev. B **87**, 020410 (2013).
- [16] S. Lounis, A. T. Costa, R. B. Muniz, D. L. Mills, Phys. Rev. Lett. **105**, 187205 (2010); S. Lounis, A. T. Costa, R. B. Muniz, D. L. Mills, Phys. Rev. B **83**, 035109 (2011).
- [17] A. T. Costa, R. B. Muniz, S. Lounis, A. B. Klautau, and D. L. Mills, Phys. Rev. B **82**, 014428 (2010).
- [18] B. Rousseau, A. Eiguren, A. Bergara, Phys. Rev. B **85**, 054305 (2012).
- [19] S. Lounis, B. Schweflinghaus, M. dos Santos Dias, M. Bouhassoune, R. B. Muniz, A. T. Costa, Surface Science **630**, 317 (2014).
- [20] R. B. Muniz, D. L. Mills, Phys. Rev. **68**, 224414 (2003).
- [21] B. Schweflinghaus, M. dos Santos Dias, A. T. Costa, S. Lounis, Phys. Rev. B **89**, 235439 (2014).
- [22] J. H. E. Griffiths, Nature **158**, 670 (1946).
- [23] C. Kittel, Phys. Rev. **71**, 270 (1947); **73**, 155 (1948).
- [24] J. H. Van Vleck, Phys. Rev. **78**, 266 (1950).
- [25] M. Farle, Rep. Prog. Phys. **61**, 755 (1998).
- [26] D. L. Mills, P. Lederer, Phys. Rev. **160**, 590 (1967).
- [27] E. K. U. Gross and W. Kohn, Phys. Rev. Lett. **55**, 2850 (1985); E. Runge and E. K. U. Gross, Phys. Rev. Lett. **52**, 997 (1984).
- [28] F. Aryasetiawan, K. Karlsson, Phys. Rev. B **60**, 7419 (1999).
- [29] C. Heil, H. Sormann, L. Boeri, M. Aichhorn, W. von der Linden, Phys. Rev. B **90**, 115143 (2014).
- [30] I. Garate, A. MacDonald, Phys. Rev. B **79**, 064403 (2009).
- [31] V. Kambarsky, Czech. J. Phys. **26**, 1366 (1976); V. Kambarsky, Phys. Rev. B **76**, 134416 (2007).
- [32] M.C. Vickey, J. S. Moodera, Phys. Rev. Lett. **102**, 137601 (2009).
- [33] T. L. Gilbert, IEEE Trans. Magn. **40**, 3443 (2004).
- [34] M. Fähnle, D. Steiauf, Phys. Rev. B **73**, 184427 (2006).
- [35] A. Brataas, Y. Tserkovnyak, G. E. W. Bauer, Phys. Rev. Lett. **101**, 037207 (2008); Y. Tserkovnyak, E. M. Hankiewicz, G. Vignale, Phys. Rev. B **79**, 094415 (2009).
- [36] A. K. Starikov, P. J. Kelly, A. Brataas, Y. Tserkovniak, G. E. W. Bauer, Phys. Rev. Lett. **105**, 236601 (2010).
- [37] H. Ebert, S. Mankovsky, D. Ködderitzsch, P. J. Kelly, Phys. Rev. Lett. **107**, 066603 (2011).
- [38] K. Gilmore, I. Garate, A. H. MacDonald, M. D. Stiles, Phys. Rev. B **84**, 224412 (2011).
- [39] Z. Qian, G. Vignale, Phys. Rev. Lett. **88**, 056404 (2002).
- [40] E. L. Wolf, D. L. Losee, Surface Science **29A**, 334 (1969).
- [41] Y.-H. Zhang, S. Kahle, T. Herden, C. Stroh, M. Mayor, U. Schlickum, M. Ternes, P. Wahl, K. Kern, Nature Communications **4**, 2110 (2013).
- [42] F. Delgado, C. F. Hirjibehedin, J. Fernandez-Rossier, Surface Science **630**, 337 (2014).
- [43] N. Papanikolaou, R. Zeller, P. H. Dederichs, J. Phys.: Condens. Matter **14**, 2799 (2002).
- [44] M. dos Santos Dias, B. Schweflinghaus, S. Blügel, S. Lounis, submitted (2014).
- [45] A. I. Lichtenstein, M. I. Katsnelson, V. P. Antropov, V. A. Gubanov, J. Magn. Magn. Mat. **67**, 65 (1987).
- [46] S. Lounis, P. H. Dederichs, Phys. Rev. B **82**, 180404(R), (2010).
- [47] A. Szilva, M. Costa, A. Bergman, L. Szunyogh, L. Nordström, O. Eriksson, Phys. Rev. Lett. **111**, 127204 (2013).
- [48] L. Bergqvist, A. Taroni, A. Bergman, C. Etz, O. Eriksson, Phys. Rev. B **87**, 144401 (2013).
- [49] D. S. G. Bauer, Ph. Mavropoulos, S. Lounis, S. Blügel, J. Phys.: Condens. Matter **23**, 394204 (2011).
- [50] D. Böttcher, A. Ernst, J. Henk, J. Phys.: Condens. Matter **23**, 296003 (2011).
- [51] This topic is the subject of a future publication.